Reversible mechanochromic and thermochromic luminescence switching *via* hydrogen-bond-directed assemblies in a zinc coordination complex†

Rui Zou,[a] Jie Zhang,*[a] Shuzhi Hu,[a] Fei Hu,[a] Haoyu Zhang[a] and Zhiyong Fu (iD) *[ab]

A bifunctional luminescent switch is constructed by introducing a terpyridyl derivative into a hydrogen-bond-assisted layered assembly structure. It exhibits interesting mechanochromic and thermochromic luminescence behaviors with reversible color changes visible to the naked eye from pink to blue-purple upon mechanical grinding and from pink to blue upon heating.

Mechanochromic and thermochromic materials sensitive to mechanical and thermal stimuli have attracted extensive interest for their promising applications in mechanical and thermal sensors, deformation detectors, security systems, and memory devices.[1] These complexes exhibit reversible modification of the emission wavelength in response to external stimuli such as light, mechanical force, heat and pH.[2] The origin of the mechanochromism has been attributed to structural changes of the constituted units, especially the molecular packing associated with intermolecular interactions such as π–π, hydrogen bond, and hydrogen bonding interactions, which influence the emissive states.[3] Reverse luminescence changes can be achieved under solvent fuming or thermal stimulus if the mechanical force only weakens the intermolecular interactions without causing any bond breakages.[4] Crystal engineering is an important part of materials science, which establishes a rapid gateway to govern the assembly of functional units and thus gain better understanding of the structure–property relationship of mechanochromic materials.[5] Nowadays, most of the

reversible mechanochromic examples reported so far are based on organic complexes.[6] By comparison with the topical research on them, the exploration of mechanochromic materials based on metal–ligand complexes is still limited.[7] Since metal coordination provides a facile way of combining different components and increases the thermal stability of the constructing motif,[8] it may give an opportunity to construct multifunctional chromic materials. Concerning nitrogen-containing heterocycles that are well known as light-sensitive components[9] and electron-deficient heterocyclic rings that have been proven to be well suited to give rise to strong π–π interactions because of their low π-electron density,[10] herein a terpyridyl derivative molecule, 4′-(4-pyridyl) 2,2′:6′,2″-terpyridine (PYTPY), with a conjugated aromatic ring system and strong luminescence emission at 375 nm (Fig. S1, ESI†) is selected as a ligand to build new stimuli-responsive metal–ligand complexes with intriguing properties. According to Kitaigorodskii's close-packing principle[11] and Etter's first hydrogen-bond rule,[12] two useful concepts for the prediction of reversible mechanochromic materials,[13] the structure of compound **1** [Zn(PYTPY)(BDC)]·3H$_2$O (BDC = 1,3-benzenedicarboxylate) is designed and constructed to incorporate these two strongly demanding factors for molecular packing, a planar aromatic core and multiple hydrogen-bonding sites. At room temperature, its crystals exhibit a significant change in solid state emissions from pink to blue-purple upon mechanical grinding and also show modification in thermochromic luminescence properties from pink to blue. This compound recovers its original crystalline phase and emission properties upon exposure to water vapor. These optical characteristics and PXRD data before and after the grinding process suggest that the mechanochromic behaviour is associated with the modification of molecular packing and the influence of fragmental interactions.

Pink crystalline powder of **1** was obtained by mixing ZnCl$_2$, PYTPY, H$_2$BDC and water at 160 °C under hydrothermal conditions. Single-crystal X-ray diffraction analysis indicates that the luminescent switch contains a one-

[a] *Key Lab for Fuel Cell Technology of Guangdong Province, School of Chemistry and Chemical Engineering, South China University of Technology, Guangzhou, Guangdong, 510640, P. R. China. E-mail: cejzhang@scut.edu.cn, zyfu@scut.edu.cn; Fax: +86 20 8711 2965*
[b] *State Key Laboratory of Photocatalysis on Energy and Environment, Fuzhou University, Fuzhou, 350002, P. R. China*

dimensional coordination polymer chain $[Zn(PYTPY)(BDC)]_n$ and solvate water molecules. The Zn(II) ion has a distorted pyramidal environment with three chelated PYTPY nitrogen atoms and two carboxylate oxygen atoms of the BDC ligand (Fig. 1a). The carboxylate arms of the BDC ligands connect the adjacent Zn(II) ions to form a one-dimensional coordination polymer. The nitrogen-containing heterocyclic PYTPY molecules are attached to the main chain as side groups (Fig. 1b). The hanging PYTPY side groups of the neighbouring chains are arranged in a face-to-face mode with the distance varying from 3.446(2) to 3.857(1) Å (Fig. 1c), showing close packing with strong π–π interactions between the aromatic rings. Solvent water molecules are located between the layers of the coordination polymers, which form multiple hydrogen bonds with neighbouring water molecules and the uncoordinated nitrogen atom of the PYTPY ligand (Fig. S2, ESI†). The weak interactions extend the final structural motif of **1** to a 3D supramolecular motif. These structural features satisfy the requirement of Kitaigorodskii's close-packing principle and Etter's first hydrogen-bond rule for the construction of mechanochromic materials.

The mechanochromic luminescence properties are revealed by grinding the solid sample in a mortar for 30 min.
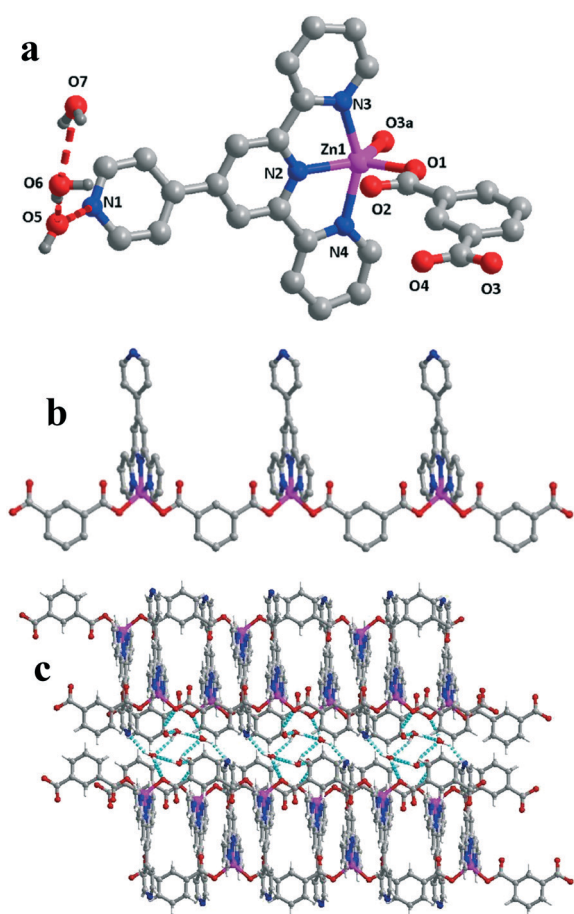

Fig. 1 The crystal structure of **1**: (a) the asymmetric unit, (b) view of the polymeric chain with PYTPY side groups and (c) the packing diagram.

Compound **1** gives pink emission at room temperature upon 365 nm UV irradiation. It is converted into much more intense blue-purple emission after grinding (Fig. 2). Upon exposure to steam, the compound reverted to its initial pink emissive phase. The process can be reproduced when the solid is ground one more time, indicating a completely reversible phenomenon. The modification of thermochromic luminescence properties is similar to its mechanochromic phenomenon. After heating above 120 °C for 30 min, the luminescence of **1** changes from pink to blue emission. The process is also reversible when the sample is treated upon exposure to steam. In addition, the sample after grinding can tune its luminescence emission from blue-purple to blue upon heating above 120 °C for 30 min, showing an interesting luminescence changing cycle. To further study the influence of grinding and heating on the crystal structure and the luminescence reversible switching behaviours, photoluminescence spectra, excited-state lifetimes, solid state UV-vis spectra, powder X-ray diffraction (PXRD) patterns and infrared spectra before and after grinding are obtained at room temperature.

It is known that electronically saturated transition metal centers coordinated with rigidity conjugated ligands can form highly emissive materials due to bond vibration or electron transfer.[14] The terpyridyl derivative (PYTPY) chelating with the zinc cation exhibits pink luminescence due to the dual emission with a strong peak at 391 nm and a weak peak at 605 nm upon 345 nm excitation in the crystalline state (Fig. 3). The emission peak of 391 nm may be assigned to the π–π* intraligand emission of PYTPY ligands, and the emission band at 605 nm is related to the intramolecular charge transfer emission.[15] After grinding, the emission band at 605 nm disappeared, while the emission peak at 391 nm red shifted to 393 nm is due to the enhanced π–π* intraligand emission of PYTPY ligands, which results in the luminescence color changing to blue-purple. The peak is restored to the initial state after the sample is treated with water vapor. The UV spectra, PXRD data and IR spectra all indicate the same trend of changes as that of fluorescence spectra. As
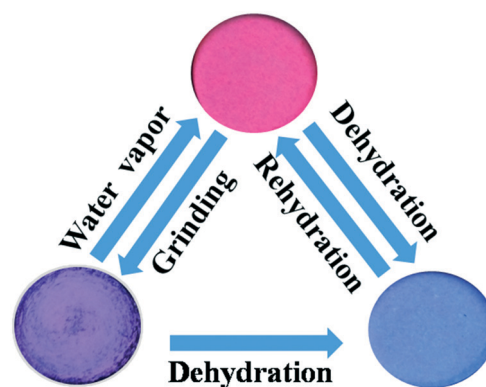

Fig. 2 Photographs of crystalline powder of **1** at different treatment conditions under UV irradiation at 365 nm (UV lamp) at room temperature.
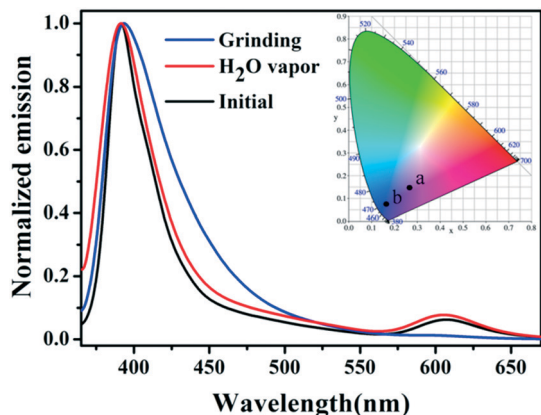
Fig. 3 Solid state fluorescence spectra of **1** before and after grinding and after being treated with water vapor. Inset: the CIE chromaticity coordinates: (a) initial sample (0.2645, 0.1461) and (b) ground sample (0.1663, 0.0814).
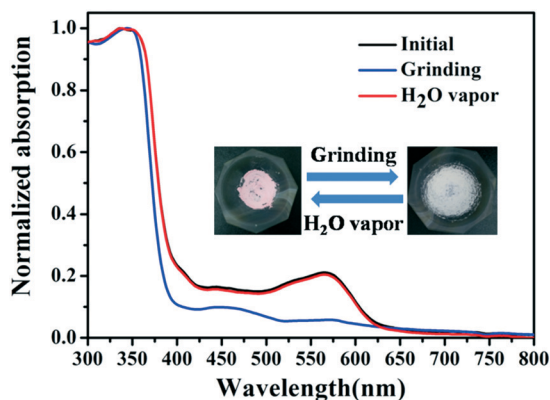

Fig. 4 UV-vis diffuse-reflectance spectra of **1** before and after grinding and after being treated with water vapor.

shown in Fig. 4, the solid state diffuse reflectance spectrum of **1** shows two absorption bands at 350 nm and 565 nm. The band that appears at 350 nm can be assigned to the π–π* transitions of the pyridine moieties, while the absorption at 565 nm contributed to the charge transfer band. After grinding, the characteristic broad band at around 565 nm disappeared, and the color of **1** turned to white. This phenomenon can be attributed to the disruption of crystal packing and the changes of hydrogen bonding interactions between the water molecules and the PYTPY ligands. The recovery of the peak at 565 nm is observed accompanied by the reverse reaction. The phase purity of the as-synthesized bulky sample was verified by the powder X-ray diffraction (PXRD) data (Fig. 5). No new diffraction peak appears, indicating that no new crystalline phase is formed during the grinding process. However, the intensities of the diffraction peaks decrease and their widths increase, suggesting the deformation of the crystal lattice and a phase conversion from the crystalline to the amorphous phase. After water vapor treatment, the identical diagram of the initial phase confirms the reversibility of the switching properties. FTIR analysis
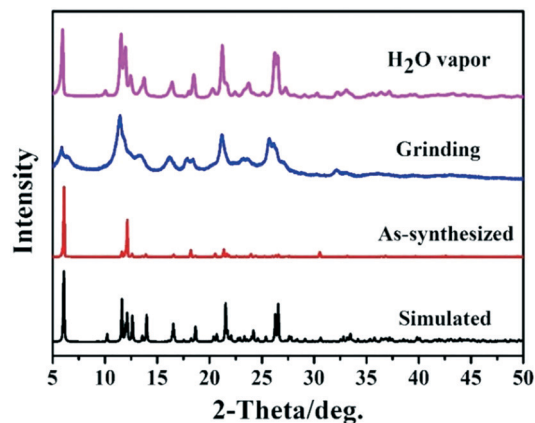

Fig. 5 PXRD data of **1** before and after grinding, simulation and being treated by water vapor.

suggests that the stretching peak of 3421 cm^{-1} red shifts to 3400 cm^{-1} after grinding, indicating the strengthening of O–H⋯O intermolecular hydrogen bonding connections involving water molecules (Fig. S3, ESI†).

The peaks in the IR spectrum also revert to the initial state after vapor treatment.

The thermochromic luminescence properties of **1** are associated with the existence of the lattice water molecules. After heating above 120 °C, the emission bands at 605 nm disappear and a new shoulder peak is distinctly observed around 475 nm accompanied by the luminescence color changing to blue (Fig. S4, ESI†). The changes in the UV and PXRD data are similar to that of mechanochromic behaviors (Fig. S5 and S6, ESI†). The diffraction peaks move towards high angles, indicating the structural shrinkage after the guest units leave. IR spectra show that the O–H stretch vibration band at 3421 cm^{-1} disappears due to the removal of water molecules (Fig. S7, ESI†). The changes in luminescence, UV, PXRD and IR data all can be restored to the initial state, showing the reversibility of the thermochromic luminescence behaviours. Emission lifetimes have been determined at room temperature. The initial emission lifetime value is 0.9572 ns, which is related to the π–π* interaction of PYTPY. It changes to 1.6625 ns and 1.5852 ns after grinding and heating, respectively, due to the weakening of multi-interactions (Fig. S8, ESI†). After dehydration, the luminescence emission color of the ground sample turns from blue-purple to blue. Its PXRD patterns correspond to those of dehydrated ones (Fig. S9, ESI†), confirming that no changes occur in the structural packing with the removal of water molecules. The emission band changes are caused by the structure collapse of the hydrogen-bonding network. TG data of the intact sample indicate that the first weight loss of 7.88% happened at 80 °C which corresponds to the loss of lattice water (calcd 7.81%) (Fig. S10, ESI†). By comparison, the leaving of water molecules takes place above 110 °C for the ground sample. This can be ascribed to the close packing after grinding, which increases the leaving temperature of water molecules. The second weight loss occurs at 410 °C and 340 °C for the intact sample

and the ground sample, respectively, accounting for the final collapse of the coordination framework. The higher collapse temperature of the intact sample is due to its better crystalline structure. Stable reversible cycles are observed for this bifunctional stimuli-responding luminescent switch, which do not show any decay for at least four rounds (Fig. S11, ESI†).

Conclusions

A new reversible luminescence switch presenting both mechanochromic and thermochromic behaviours has been synthesized and characterized. Its stable photoactive framework is built *via* attaching the nitrogen containing heterocyclic units to a zinc benzenedicarboxylate chain. The structural arrangements provide close packing and multi-interactions between the adjacent groups. The luminescence origin of the MOF-based switch has been established based on the experimental data. The modulation of the photoluminescence properties by means of external stimuli is particularly attractive for constructing photo-responding materials. Although many examples of mechanochromic compounds have been reported, the system based on simple coordination polymers has rarely been reported. Mechanochromic compounds built in this way avoid the tedious synthesis of organic systems. In view of the previously successful preparation of numerous mixed-ligand metal–organic frameworks, it is applicable to design and construct a large variety of mechanochromic and thermochromic switches by using crystal engineering principles.

Conflicts of interest

There are no conflicts of interest to declare.

Acknowledgements

Notes and references

1 (a) H. Sun, S. Liu, W. Lin, K. Y. Zhang, W. Lv, X. Huang, G. Jenkins, Q. Zhao and W. Huang, *Nat. Commun.*, 2014, **5**, 3601; (b) D. Genovese, A. Aliprandi, E. A. Prasetyanto, M. Mauro, M. Hirtz, H. Fuchs, Y. Fujita, H. UjiI, S. Lebedkin, M. Kappes and L. De Cola, *Adv. Funct. Mater.*, 2016, **26**, 5271; (c) Y. H. Han, C. B. Tian, Q. H. Li and S. W. Du, *J. Mater. Chem. C*, 2014, **2**, 8065.

2 (a) Q. Zhu, T. Sheng, C. Tan, S. Hu, R. Fu and X. Wu, *Inorg. Chem.*, 2011, **50**, 7618; (b) S. Perruchas, X. F. Le Goff, S. Maron, I. Maurin, F. Guillen, A. Garcia, T. Gacoin and J. P. Boilot, *J. Am. Chem. Soc.*, 2010, **132**, 10967; (c) G. M. Espallargas, L. Brammer, J. Van de Streek, K. Shankland,

A. J. Florence and H. Adams, *J. Am. Chem. Soc.*, 2006, **128**, 9584.

3 (a) Y. Sagara, T. Mutai, I. Yoshikawa and K. Araki, *J. Am. Chem. Soc.*, 2007, **129**, 1520; (b) B. Xu, H. Wu, J. Chen, Z. Yang, Z. Yang, Y. C. Wu, Y. Zhang, C. Jin, P. Y. Lu, Z. Chi, S. Liu, J. Xu and M. Aldred, *Chem. Sci.*, 2017, **8**, 1909; (c) H. Wu, C. Hang, X. Li, L. Yin, M. Zhu, J. Zhang, Y. Zhou, H. Ågren, Q. Zhang and L. Zhu, *Chem. Commun.*, 2017, **53**, 2661; (d) X. Zhang, J. Y. Wang, D. Qiao and Z. N. Chen, *J. Mater. Chem. C*, 2017, **5**, 8782; (e) Y. Yan, N. N. Zhang, R. Li, J. G. Xu, J. Lu, F. K. Zheng and G. C. Guo, *Eur. J. Inorg. Chem.*, 2017, **32**, 3811; (f) Q. Benito, X. F. Le Goff, S. Maron, A. Fargues, A. Garcia, C. Martineau, F. Taulelle, S. Kahlal, T. Gacoin, J. P. Boilot and S. Perruchas, *J. Am. Chem. Soc.*, 2014, **136**, 11311.

4 (a) J. F. Chen, D. P. Gong, J. Wen, H. Ma and D. K. Cao, *Chem. Sci.*, 2016, **7**, 451; (b) S. S. Zhao, L. Chen, L. Wang and Z. Xie, *Chem. Commun.*, 2017, **53**, 7048.

5 (a) Q. Zhang, J. Su, D. Feng, Z. Wei, X. Zou and H. C. Zhou, *J. Am. Chem. Soc.*, 2015, **137**, 10064; (b) Q. Benito, I. Maurin, M. Poggi, C. Martineau-Corcos, T. Gacoin, J. P. Boilot and S. Perruchas, *J. Mater. Chem. C*, 2016, **4**, 11231.

6 Y. Sagara, S. Yamane, M. Mitani, C. Weder and T. Kato, *Adv. Mater.*, 2016, **28**, 1073.

7 (a) O. Toma, M. Allain, F. Meinardi, A. Forni, C. Botta and N. Mercier, *Angew. Chem.*, 2016, **128**, 8130; (b) M. S. Deshmukh, A. Yadav, R. Pant and R. Boomishankar, *Inorg. Chem.*, 2015, **54**, 1337; (c) P. Xue, J. Ding, P. Wang and R. Lu, *J. Mater. Chem. C*, 2016, **4**, 6688; (d) Y. Yan, J. Chen, N. N. Zhang, M. S. Wang, C. Sun, X. S. Xing, R. Li, J. G. Xu, F. K. Zheng and G. C. Guo, *Dalton Trans.*, 2016, **45**, 18074.

8 (a) X. Zhang, Z. Chi, Y. Zhang, S. Liu and J. Xu, *J. Mater. Chem. C*, 2013, **1**, 3376; (b) J. Zhang, J. Geng, G. Zheng, J. Dai and Z. Fu, *Chem. Commun.*, 2014, **50**, 7326.

9 Q. Zhang, J. Chen, X. Y. Wu, X. L. Chen, R. Yu and C. Z. Lu, *Dalton Trans.*, 2015, **44**, 6706.

10 Y. Sagara and T. Kato, *Nat. Chem.*, 2009, **1**, 605.

11 A. I. Kitaigorodskii, *Organic Chemical Crystallography*, Consultants Bureau, New York, 1961.

12 M. C. Etter, *Acc. Chem. Res.*, 1990, **23**, 120.

13 (a) H. N. Wang, G. G. Shan, H. B. Li, X. L. Wang, H. T. Cao and Z. M. Su, *CrystEngComm*, 2014, **16**, 2754; (b) H. Yu, W. Ren, H. Lu, Y. Liang and Q. Wang, *Chem. Commun.*, 2016, **52**, 7387.

14 (a) J. Costa, R. Ruloff, L. Burai, L. Helm and A. E. Merbach, *J. Am. Chem. Soc.*, 2005, **127**, 5147; (b) B. C. Wang, Q. R. Wu, H. M. Hu, X. L. Chen, Z. H. Yang, Y. Q. Shang, M. L. Yang and G. L. Xue, *CrystEngComm*, 2010, **12**, 485.

15 (a) C. Chen, X. H. Jin, X. J. Zhou, L. X. Cai, Y. J. Zhang and J. Zhang, *J. Mater. Chem. C*, 2015, **3**, 4563; (b) L. Marrucci, D. Paparo, P. Maddalena, E. Massera, E. Prudnikova and E. Santamato, *J. Chem. Phys.*, 1997, **107**, 9783.